

Predictive Direct Power Control of MV Grid-connected Three-level NPC Converters

S. Aurtenechea¹, M. A. Rodríguez¹, E. Oyarbide², J. R. Torrealday¹

⁽¹⁾*Faculty of Engineering, University of Mondragon, Loramendi 4, Aptdo. 23, 20500 Arrasate, Spain*

saurtenetxea@eps.mondragon.edu, marodriguez@eps.mondragon.edu, jrtorrealday@eps.mondragon.edu

⁽²⁾*Aragón Institute for Engineering Research (I3A), University of Zaragoza, María de Luna 1, 50018 Zaragoza, Spain*
eoyerabid@unizar.es

Abstract-This paper deals with an improvement of the Predictive Direct Power Control (P-DPC) for MV three-level NPC converters. Contrary to the previously developed P-DPC strategy, the proposed approach combines a symmetrical 3+3 voltage vectors' sequence for the steady-state operation with a simple two voltage vectors' sequence for transient requirements. Simulations of the proposed hybrid algorithm are compared to a standard Voltage Oriented Control (VOC) under 2.3kV-2MVA operation conditions. Both the P-DPC and the VOC strategies offer similar steady-state performances but the P-DPC is clearly better during transients. These results match with the expected behavior and reinforce the choice of P-DPC as an attractive candidate for the control of MV grid connected converters.

I. INTRODUCTION

The development of new kinds of high voltage and fast switching semiconductors (as Integrated Gate Commutated Thyristors, IGBTs, High Voltage IGBTs, HV-IGBTs etc.) combined with the utilization of Digital Signal Processors (DSPs) has stimulated the connection of power converters to Medium Voltage (MV) levels [1]. Direct MV connection is commonly required in industrial drives, renewable-energy generation systems and power quality improvement units (FACTs or D-FACTS) [1-3]. Multilevel converters and particularly three-level Neutral Point Clamped (NPC) Voltage-Source Inverters (VSIs) are commonly used in many of these applications [4]. These topologies offer reduced voltage ratings of the switches and good harmonic spectrum in the AC-side, which lead to an attractive optimum between performance and cost for MV grid connection.

Nowadays, the common way of connecting high-power VSIs to the MV grid is by means of a coupling transformer, in such a way that the well known and mature Low-Voltage (LV) inverter technology can be exploited. This configuration leads to good steady-state and transient behaviors [2]. However, the coupling transformer penalizes the global efficiency and usually presents a bulky size. Hence, it could be of interest to take advantage of the state-of-the-art of new semiconductors combined with multilevel topologies, getting a transformerless direct MV connection [3]. In a similar way, there is a trend to use these new devices in the update of old power systems (commonly based on conventional technologies as Thyristors and GTOs), getting higher switching frequencies [1].

This paper is focused on the control of active and reactive power-flows of transformerless grid-connected three-level NPC VSIs. After a brief presentation of commonly used control schemes, a new control approach for the three-level NPC converter is proposed: the Predictive Direct Power Control (P-DPC). Next, one of the possible approaches of the P-DPC is developed. Finally, several comparative simulations of a grid connected three-level NPC VSI under the P-DPC and Voltage Oriented Control are discussed.

II. CONTROL STRUCTURES OF GRID-CONNECTED DC/AC CONVERTERS

Generally, these devices must provide a target active and/or reactive power to the line, so appropriate Power Control is required [5]. The control techniques which are commonly used in grid connected converter systems could be classified as direct or indirect control strategies, see Fig.1 [6,7]. The indirect control is characterized by a modulator (Pulse Width Modulation PWM or other) that computes the turn-on/turn-off times of converter's switches along a switching period through the evaluation of the voltage reference. This voltage reference is issued by the controller, which idealizes the converter as a dependent continuous voltage source. On the other hand, direct control techniques establish a direct relation between the behavior of the controlled variable and the state of the converter's switches.

Though there are many strategies to control the grid-side converters, summarized in Fig.1, the indirect-control type Voltage Oriented Control (VOC) is mainly utilized [5-7]. It is based on the knowledge of the position of the line-voltage vector and the relative spatial orientation of the current vector. It employs the well-known Park's transformation to a rotating $dq0$ reference frame (aligned with the line-voltage) or the Clark's transformation to a static $\alpha\beta0$ reference frame. Generally, it presents two cascaded control loops in such a way that a fast inner loop controls the grid current and an external loop the DC-link voltage. This control strategy generally leads to good transient behaviors and acceptable steady-state operation. It operates at a constant switching frequency, which facilitates the use of advanced modulation techniques, simplifies the line-side filter design and improves conversion efficiency.

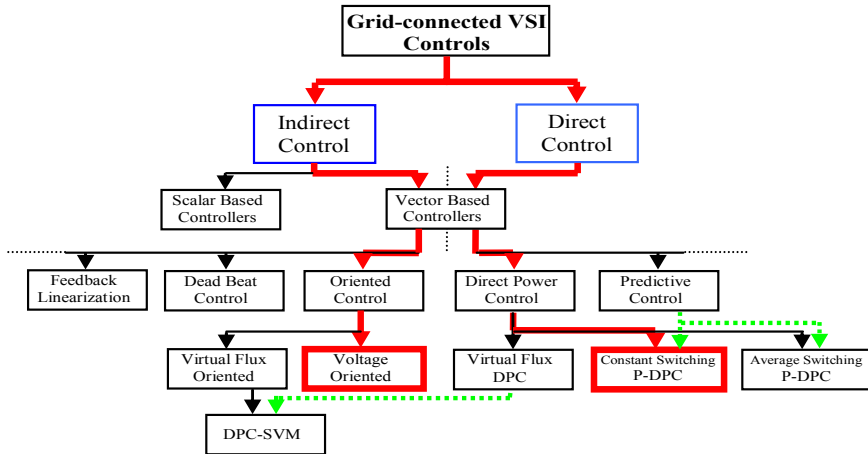


Fig.1. Classification of Grid-connected VSI controls

On the other hand, direct control strategies offer faster transients and robust behavior against system variations. However, its basic formulations lead to variable switching frequency and/or non-optimized conversion efficiency levels in grid-connected converters [8]. There are several approaches trying to solve these disadvantages, and among them, the so-called Predictive Direct Power Control (P-DPC) has been recently proposed [6-7]. In this new proposal, a predictive approach selects a set of concatenated-voltage vectors, obtaining high-dynamic responses in large-transients under a constant switching frequency. The set of concatenated-voltage vectors of the P-DPC can be built in different forms, combining different design criteria such as conversion efficiency, current ripple or others.

This paper extends the basic formulation of the P-DPC of [6-7] to the case of three-level NPC converters, leading to a new hybrid P-DPC version. The main idea is to make use of a large set of concatenated-voltage vectors in steady state operation, thus improving efficiency and current ripple, and to exploit the advantages of a simple set of two concatenated-voltage vectors in transients.

III. PREDICTIVE DIRECT POWER CONTROL. THEORY AND APPLICATION TO A THREE-LEVEL NPC VSI

The P-DPC selects the voltage-vectors' sequences and computes their application times in order to control the power flow through the VSI under a constant switching frequency operation. This strategy requires a predictive model of the instantaneous active (P) and reactive (Q) power time-derivative behaviors (1), which is explained in [6-7] for a generic VSI with an L-type inductive filter.

$$\begin{aligned} \frac{dP}{dt} &= v_\alpha \left(\frac{1}{L} (v_{K\alpha} - v_\alpha) + \omega i_\beta \right) + v_\beta \left(\frac{1}{L} (v_{K\beta} - v_\beta) - \omega i_\alpha \right) \\ \frac{dQ}{dt} &= v_\alpha \left(\omega i_\alpha - \frac{1}{L} (v_{K\beta} - v_\beta) \right) + v_\beta \left(\frac{1}{L} (v_{K\alpha} - v_\alpha) + \omega i_\beta \right) \end{aligned} \quad (1)$$

In (1) $v_{\alpha\beta}$, $v_{K\alpha\beta}$ and $i_{\alpha\beta}$ are the line voltage, converter's voltage and line current in static $\alpha\beta$ coordinates. As it can be observed the power time-derivative values depend on the grid

variables, filter inductors and on the state of converter's switches.

Fig.2 shows the basic scheme of a grid-connected three-level NPC VSI with an L-type filter. The converter is built around twelve switching cells (based on IGBTs, IGCTs, or others) and six clamp diodes. This configuration leads to 27 possible switching states, related to 19 possible voltage vectors at the output of the converter, see Fig.3.

The output of the VSI is considered constant during each voltage-vector application $v_k = [v_{ka} \ v_{kb}]^T$. In the same way, if the switching frequency is high enough, it can be assumed that the line voltage $v = [v_a \ v_b]^T$ is also kept constant during the same period.

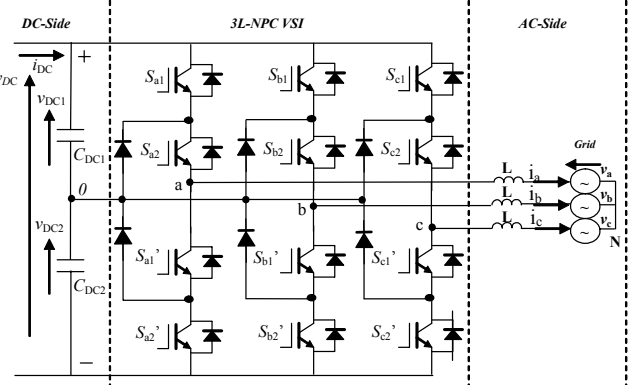


Fig.2. Grid-connection of a three-phase 3L-NPC VSI with an L-type filter

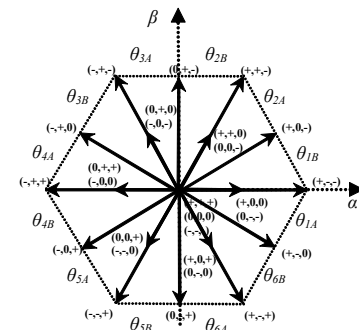


Fig.3. Space vector representation of the available voltage vectors at the AC-side of the converter

Thus, and provided that current variations are small, quasi-constant active and reactive power behaviors can be derived during each voltage-vector application. These assumptions allow simple geometrical analysis of concatenated power trajectories. The slopes of the variations of active and reactive powers during a voltage-vector application are defined as follows:

$$\begin{aligned} f_{pi} &= \frac{dP}{dt} \Big|_{\vec{v}_k=\vec{v}_i} \\ f_{qi} &= \frac{dQ}{dt} \Big|_{\vec{v}_k=\vec{v}_i} \end{aligned} \quad (2)$$

With i denoting the position index of the applied voltage in the sequence of voltage-vectors. Equation (3) computes linear trajectories of active and reactive powers under a given voltage-vector application during the related application time.

$$\begin{aligned} P_i &= P_{i-1} + f_{pi} t_{ai} \\ Q_i &= Q_{i-1} + f_{qi} t_{ai} \end{aligned} \quad (3)$$

with $\{P_{i-1} Q_{i-1}\}$ the initial active and reactive power values in the beginning of the i -th vector of the sequence, t_{ai} the application time and $\{P_i Q_i\}$ the active and reactive power values at the end of the application time.

The P-DPC strategy is based on the concatenation of several (3)-type trajectories along the control period, leading to the so-called voltage-vectors' sequence. This concatenation can be carried out in different ways, e.g. it can result in a non-symmetrical switching pattern containing two or three voltage vectors, or it can provide a symmetrical switching pattern combining two or three vectors, leading to a 2+2 or 3+3 type voltage-vectors' sequence [6-7].

A. Steady-State Operation. P-DPC based on a symmetrical 3+3 vectors' sequence

In the case of steady-state operation, a symmetrical 3+3 switching pattern is used. The voltage-vectors' sequence is divided in two sub-sequences of three voltage-vectors each, see Fig. 4. The second subsequence is symmetrical to the first one, i.e., it is built by the same voltage-vectors and employs the same application times but reverses the application order. Thus, the last voltage vector of the first sequence matches up with the first voltage vector of the second sequence, leading to a switching frequency minimization. Fig. 4 shows an example of the concatenation of different power-trajectories in a steady-state case during two control periods. In the beginning of each control period the algorithm must select three of the applicable voltage vectors, computing then the required application times.

1) Voltage Vectors' Selection: In the field of three level NPC converters, the “nearest-three-vector” (NTV) vector-selection criteria is widely used in the space vector modulation (NTV-SVM) under VOC-type control strategies [4,9]. This criteria minimizes the number of commutations, improves the power quality and minimizes the generated electromagnetic interferences (EMIs). The work presented here exploits the NTV idea in order to choose the voltage-vectors' sequence of the P-DPC algorithm.

The line-voltage plane is divided in six sectors of 60° , $[\theta_1.. \theta_6]$, which are also divided in two sub-sectors, $[\theta_{iA}.. \theta_{iB}]$. Next, an example of vector selection will be discussed using Fig.5. This figure shows the first quadrant of the line-voltage space, composed by the half of sector 1 and entire sector 2. The analysis carried out in this quadrant can be easily extended to any other quadrant. As the use of the nearest voltage-vectors provides the smallest current ripple, when the grid voltage is located at any given sector, θ_i , each application subsequence must be built using voltage-vectors belonging to the set of large vectors $\{\vec{v}_{K1_l}, \vec{v}_{K1_l-1}, \vec{v}_{K1_l-2}\}$, medium vectors $\{\vec{v}_{K1_m}, \vec{v}_{K1_m-1}, \vec{v}_{K1_m-2}\}$, small vectors $\{\vec{v}_{K1_s}, \vec{v}_{K1_s-1}, \vec{v}_{K1_s-2}\}$ and null vectors, $\{\vec{v}_{z0}, \vec{v}_{z1}, \vec{v}_{z2}\}$. In the case of sub-sector IB , for example, next voltage application sub-sequences can be used,

$$\left. \begin{aligned} &\left[\vec{v}_{K1_m}, \vec{v}_{K1_l}, \vec{v}_{K1_s} \right] \left[\vec{v}_{K2_s}, \vec{v}_{K2_l}, \vec{v}_{K1_m} \right] \\ &\left[\vec{v}_{K1_m}, \vec{v}_{K2_s}, \vec{v}_{K1_s} \right] \left[\vec{v}_{K1}, \vec{v}_{K2_l}, \vec{v}_{K1_s} \right] \end{aligned} \right\} \quad (4)$$

The appropriate sub-sequence will depend on the optimization strategy and DC voltage stabilization requirements. The vectors' sequence is completed when the sub-sequence is symmetrically applied along control period.

2) Application Times: Equations (3) combined with the constant switching frequency constraint forms the set of equations defining the overall behavior of active and reactive powers during the voltage-vectors' sequence:

$$\begin{aligned} P_1 &= P_0 + f_{p1} \cdot 2t_{a1} & / & Q_1 = Q_0 + f_{q1} \cdot 2t_{a1} \\ P_2 &= P_1 + f_{p2} \cdot 2t_{a2} & / & Q_2 = Q_1 + f_{q2} \cdot 2t_{a2} \\ P_3 &= P_2 + f_{p3} \cdot 2t_{a3} & / & Q_3 = Q_2 + f_{q3} \cdot 2t_{a3} \\ T_{sw}/2 &= t_{a1} + t_{a2} + t_{a3} \end{aligned} \quad (5)$$

The control algorithm must compute the application times $\{t_{a1}, t_{a2}, t_{a3}\}$ in such a way that controlled variables evolve from their initial values, $\{P_0 Q_0\}$, towards the reference values, $\{P_3 Q_3\}$.

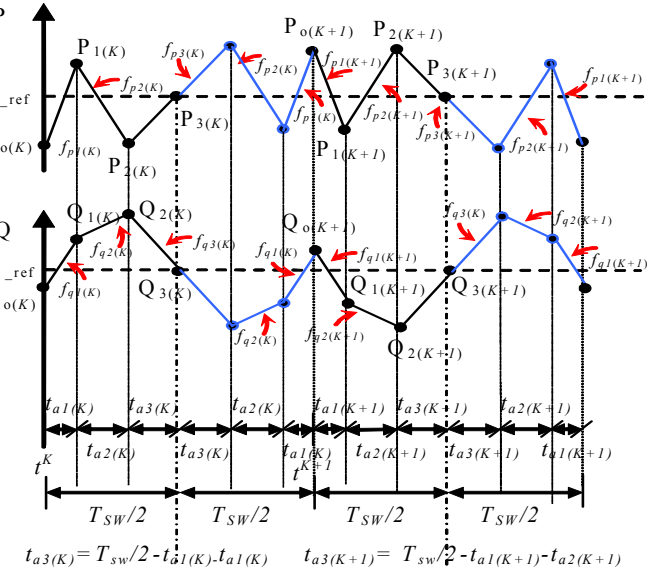


Fig.4. Example of the steady state behavior of the P-DPC strategy with a symmetrical 3+3 voltage vectors' sequence

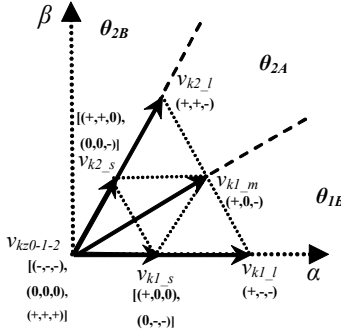


Fig.5. Set of available voltage vectors

The problem has seven equations and six variables, so an approximate solution based on some optimization criteria must be computed. The selected approach tries to minimize the active and reactive power tracking errors, which are defined as:

$$e_{Fp} = \overbrace{P_{\text{ref}} - P_0}^{e_{po}} - 2f_{p1}t_{a1} - 2f_{p2}t_{a2} - 2f_{p3}\left(\frac{T_{sw}}{2} - t_{a1} - t_{a2}\right) \quad (6)$$

$$e_{Fq} = \overbrace{Q_{\text{ref}} - Q_0}^{e_{qo}} - 2f_{q1}t_{a1} - 2f_{q2}t_{a2} - 2f_{q3}\left(\frac{T_{sw}}{2} - t_{a1} - t_{a2}\right)$$

A least-square optimization method is used, trying to minimize the weight function of equation (7).

$$F = e_{Fp}^2 + e_{Fq}^2 \quad (7)$$

The optimal set of application times that minimizes F during a control period satisfies the next two minimum value conditions:

$$\begin{cases} \frac{\partial F}{\partial t_{a1}} = 0 \\ \frac{\partial F}{\partial t_{a2}} = 0 \end{cases} \quad (8)$$

Solving the set of equations derived from (8) it is straightforward to get the next application times:

$$t_{a1} = \begin{bmatrix} (f_{q2} - f_{q3}) \cdot e_{po} + (f_{p3} - f_{p2}) \cdot e_{qo} \\ + (f_{q3} \cdot f_{p2} - f_{q2} \cdot f_{p3}) \cdot \frac{T_{sw}}{2} \end{bmatrix}$$

$$t_{a2} = \begin{bmatrix} f_{q3} \cdot f_{p2} - f_{q1} \cdot f_{p2} - f_{q2} \cdot f_{p3} \\ + f_{q1} \cdot f_{p3} - f_{q3} \cdot f_{p1} + f_{q2} \cdot f_{p1} \end{bmatrix}$$

$$t_{a3} = \begin{bmatrix} (f_{q3} - f_{q1}) \cdot e_{po} + (f_{p1} - f_{p3}) \cdot e_{qo} \\ + (-f_{q3} \cdot f_{p1} + f_{q1} \cdot f_{p3}) \cdot \frac{T_{sw}}{2} \end{bmatrix}$$

$$t_{a3} = \frac{T_{sw}}{2} - t_{a1} - t_{a2}$$

$$(9)$$

B. Transient-state Operation. P-DPC based on a two-vectors' sequence

This P-DPC version is based on the optimum concatenation of two (3)-type trajectories along the control period, which is an attractive solution for transient operations. Fig. 6 shows an example with a first steady-state switching pattern followed by an active-power-reference step. Note that reference evolutions are always conditioned to the maximum available current value, in such a way that non-predicted behaviors are avoided.

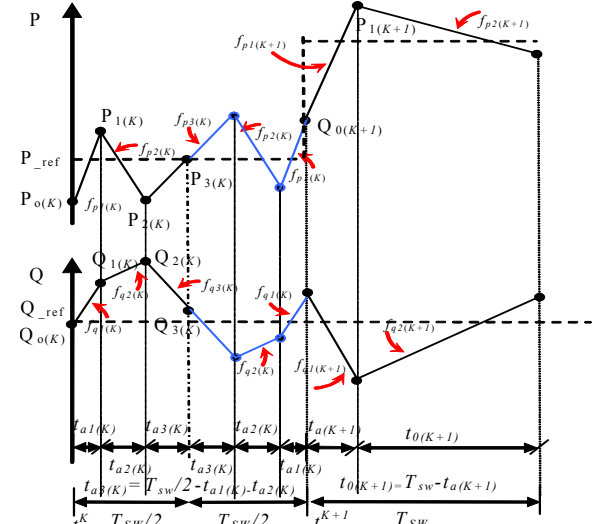


Fig.6. Example of P-DPC based on two vectors sequence algorithm behavior during an active power reference step

1) *Voltage Vectors' Selection:* A transient is simply an evolution between two different steady-states, which are defined by two different P - Q references. The target requirement is to change of state as fast as possible, regardless of efficiency, current ripple or THD constraints, which are not relevant in transients. Thus, the largest voltage vector which leads to the largest desired P - Q evolution slopes must be selected. The rest of the switching period can be completed by a null voltage-vector.

Though it would be possible to eliminate the null-vector application time, passing directly to the 3+3 steady-state switching pattern, it is not recommended if line-synchronized switching strategy is required, which is commonly used in high power conversion systems.

2) *Application Times:* Considering (3) and constant switching-frequency condition, it is possible to get the set of equations defining the overall evolution of active and reactive powers during the transient behavior (10).

$$P_1 = P_0 + f_{p1} t_a \quad / \quad Q_1 = Q_0 + f_{q1} t_a$$

$$P_2 = P_1 + f_{p2} t_0 \quad / \quad Q_2 = Q_1 + f_{q2} t_0 \quad (10)$$

$$T_{sw} = t_a + t_0$$

The control algorithm must compute the application time t_a in such a way that controlled variables evolve from their initial values, $\{P_0 Q_0\}$, towards the new reference values $\{P_2 Q_2\}$, see Fig.6. This problem has five equations and three variables, so an optimum solution similar to that used in the steady-state case must be employed. The new active and reactive power tracking errors are defined as:

$$e_{Fp} = \overbrace{P_{\text{ref}} - P_0}^{e_{po}} - f_{p1} t_a - f_{p2} (T_{sw} - t_a) \quad (11)$$

$$e_{Fq} = \overbrace{Q_{\text{ref}} - Q_0}^{e_{qo}} - f_{q1} t_a - f_{q2} (T_{sw} - t_a)$$

Using the weight function (7) defined in the previous section and solving the restriction (12) it is possible to derive the equation (13) which gives the optimal application time $[t_a]$ that minimizes the final tracking error.

$$\frac{\partial F}{\partial t_a} = 0 \quad (12)$$

$$t_a = -\frac{[-T_{sw} \cdot (f_{q2}^2 + f_{p2}^2) + T_{sw} \cdot (f_{p2} \cdot f_{p1} + f_{q2} \cdot f_{q1})] + e_{po} \cdot (f_{p2} - f_{p1}) + e_{qo} \cdot (f_{q2} - f_{q1})}{(f_{p2} - f_{p1})^2 + (f_{q2} - f_{q1})^2} \quad (13)$$

$$t_0 = T_{sw} - t_a$$

C. DC-link Balance Requirements

In steady-state operation it is important to keep the required voltage-balance in DC-link capacitors. Defining the converter's neutral-point-voltage unbalance as e_0 , which can be denoted as neutral error, its time-evolution is given by equation (14).

$$\frac{de_0}{dt} = \frac{1}{C_{DC2}} [(S_{a2} - S_{a1})i_a + (S_{b2} - S_{b1})i_b + (S_{c2} - S_{c1})i_c] \quad (14)$$

with S_{xi} the state of the switch number i belonging to the switching-leg x and i_x the line current through the phase x , see Fig. 2. Making the same assumptions as in previous sections, a quasi-constant neutral-error evolution can be considered. Therefore it is possible to carry out a simple geometrical analysis of the concatenated neutral-error trajectories. Describing the slope of the linear evolution of the neutral-error during a voltage-vector application,

$$f_{e0i} = \left. \frac{de_0}{dt} \right|_{\vec{v}_k = \vec{v}_i} \quad (15)$$

the neutral-error at the end of the switching period is obtained:

$$e_{F0} = \overbrace{v_{DC1} - v_{DC2}}^{v_o} - 2f_{e01}t_{a1} - 2f_{e02}t_{a2} - 2f_{e03}\left(\frac{T_{sw}}{2} - t_{a1} - t_{a2}\right) \quad (16)$$

The voltage vectors are selected in order to maintain the controlled $P-Q$ variables close to the reference values. The fact is that some of these voltage vectors can be obtained by different switch configurations, implying different neutral-error evolutions. This redundancy, which is especially present in the “small voltage-vectors” family, provides an additional degree of freedom which is exploited in order to minimize the neutral-error value. The control algorithm must simply retain the redundant voltage-vector that minimizes the neutral-error (16).

D. Proposed Control System Configuration

The system's block diagram and the flowchart of the proposed P-DPC technique are shown in Fig.7. Initial line voltage and current values are required in order to compute initial active and reactive powers [P_0, Q_0]. The proposed strategy evaluates this information and the reference power values, selects the appropriate sequence (steady-state or transient-state) and computes the application times which minimize the final tracking errors.

IV. SIMULATION RESULTS

In order to verify the behavior of the proposed control algorithm, several simulations comparing a VOC-type NTV-SVM with the proposed P-DPC strategy have been carried out. The specifications and parameters of the model are listed in Table I. Fig. 8 shows the line current in the steady-state which is evaluated by THD measurements. Both strategies present

TABLE I
SPECIFICATIONS OF THE GRID CONNECTED THREE PHASE VSI

Value [unit]	
Rated Power (S_k)	2 [MVA] $\cos\theta=0.9(i)$
Rated line-to-line Voltage	2.3 [kV]
Filter (L)	1.2 [mH] $\pm 10\%$
DC Link (C_{DC})	12 [mF] / 4100 [V]
Control frequency (1/T _{sw})	1500 [Hz]

similar harmonic spectrum levels, near 4.25%, meeting the IEEE Std 519-1992 recommendation. The P-DPC behavior along two control periods is shown in Fig.9a. As it can be observed, quasi-linear trajectories evolve around the reference values, with a ripple of around 5%. Figure 9b shows the evolutions of the DC-link voltages and the neutral-error under P-DPC operation. This figure shows a perturbation located at the typical frequency of 150Hz, characteristic of three-level converters with some kinds of SVMs. Finally, the active and reactive power transient behaviors under several active-power steps of 600kW (30% S_k) are shown in Fig.10. The PI controllers of the VOC strategy (based on Park's dq Transformation) are tuned using optimal approaches, leading to a fast transient response of around 15ms [5]. However, it is possible to observe a substantial overshoot and the dq cross-coupling effect. On the other hand, the P-DPC strategy shows an improved transient behavior, obtaining a fast dynamic response below 3ms without any overshoot neither cross-coupling effects.

V. CONCLUSIONS

An improvement of the P-DPC has been proposed. This new approach exploits a symmetrical 3+3 voltage-vectors' sequence on steady-state operation and a simple but fast sequence of 2 voltage-vectors for transient purposes. It has been compared to a VOC-based NTV-SVM strategy, showing a similar performance level in steady-state operation but improving the transient behavior. These results are coherent with the fact that both strategies exploit the same set of voltage-vectors in steady-state operation and that the $d-q$ cross-coupling affects to VOC-based systems in transients. In addition, this paper presents a first P-DPC application to a three-level VSI. In order to get the required voltage-balance of DC-link capacitors, a new P-DPC of the neutral voltage evolution has been achieved. These first promising results place the P-DPC strategy as a good candidate for power control purposes.

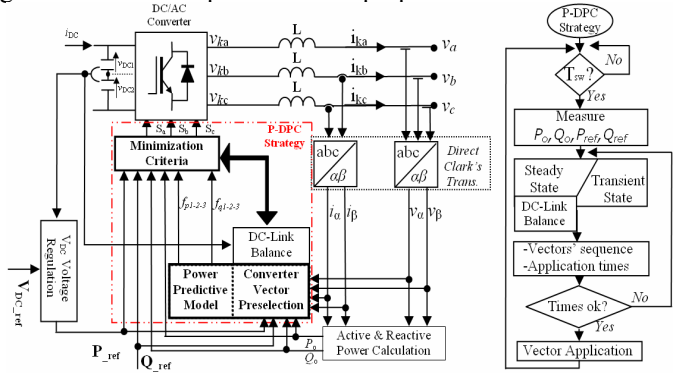


Fig.7. System's block diagram and control flowchart of the P-DPC strategy

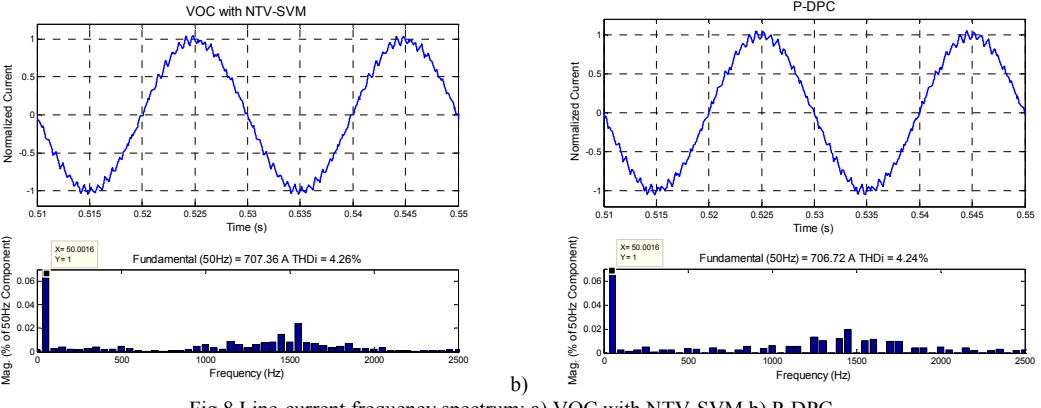


Fig.8 Line-current frequency spectrum: a) VOC with NTV-SVM b) P-DPC

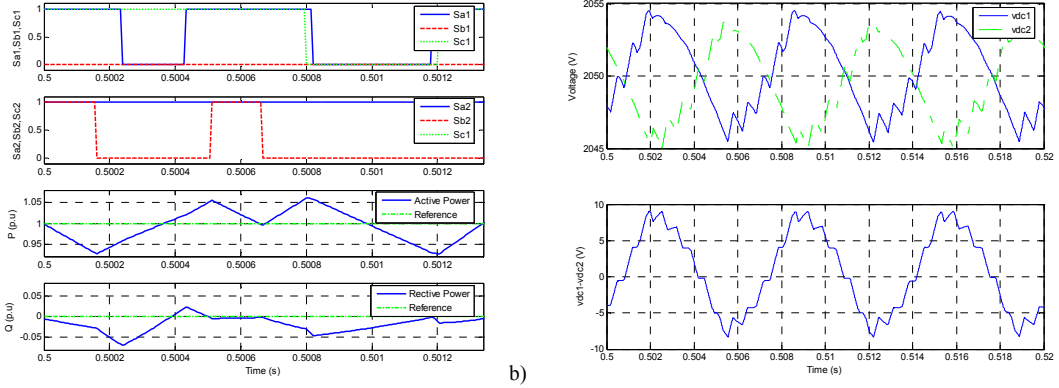


Fig.9 a) Switching signals and active and reactive power trajectories along two control periods under the P-DPC operation, b) DC-link voltages and error in the neutral point under the P-DPC operation

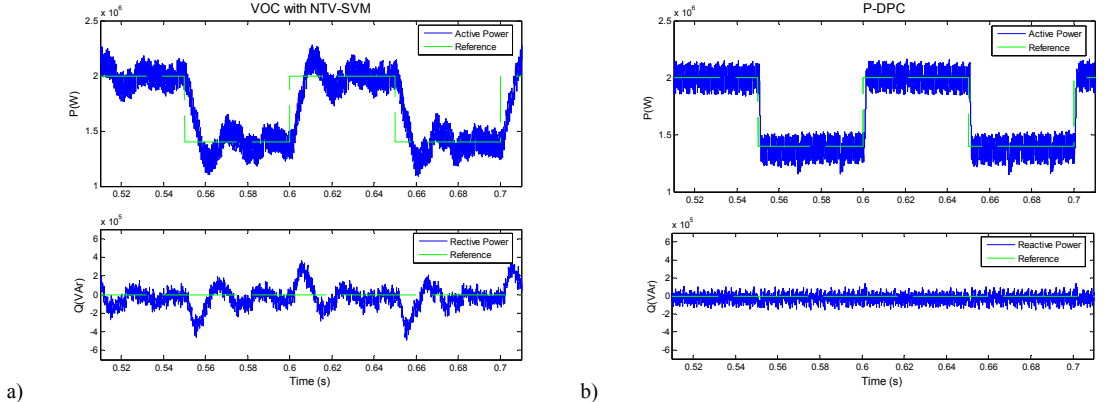


Fig.10. Instantaneous active and reactive power during several active power reference steps: a) VOC with NTV-SVM b) P-DPC

ACKNOWLEDGMENT

This work has been supported by the programs: Investigación Básica y Aplicada (PI 2003-11) and Formación de Investigadores del Dpto. de Educación, Universidades e Investigación from the Basque Government and by ENE2005-09218-C02-00 from MCYT DGI/FEDER.

REFERENCES

- [1] S. Bernet, "State of The Art and Developments of Medium Voltage Converters", Proceedings of PELINCEC 2005, Warsaw, Poland.
- [2] F. Blaabjerg, T. Teodorescu, M. Liserre, A. V. Timbus, "Overview of Control and Grid Synchronization for Distributed Power Generation Systems", IEEE Trans. Industrial Electronics, vol 53, Oct. 2006, pp.1398-1409.
- [3] S. Alepuz, S. Busquets-Monge, J. Bordonau, J. Gago, D. González, J. Balcells, "Interfacing Renewable Energy Sources to the Utility Grid Using a Three-Level Inverter", *IEEE Trans. Industrial Electronics*, vol 53, Oct. 2006, pp.1504-1511.
- [4] J. Rodriguez, J.-S. Lai and F. Z. Peng, "Multilevel Inverters: A Survey of Topologies, Controls and Applications", *IEEE Trans. Industrial Electronics*, vol 49, August. 2002, pp.724-738.
- [5] M. P. Kazmierkowski, R. Krishnan and F. Blaabjerg, "Control in Power Electronics", *Academic Press*, 2002.
- [6] S. Aurtenechea, M. A. Rodriguez, E. Oyarbide, J. R. Torrealday, "Predictive Direct Power Control-A New Control Strategy for DC/AC Converters", *Proceedings of IECON 2006*, Paris, France.
- [7] S. Aurtenechea, M. A. Rodriguez, E. Oyarbide, J. R. Torrealday, "Predictive Control Strategy for DC/AC Converters Based on Direct Power Control", *IEEE Trans. Industrial Electronics*, "In Press".
- [8] P. Antoniewicz, "Predictive Direct Power Control of a Rectifier", *Proceedings of PELINCEC 2005*, Warsaw, Poland.
- [9] B.P. McGrath, D.G. Holmes, T. Lipo, "Optimized space vector switching sequences for multilevel inverters", *IEEE Trans. Power Electronics*, vol. 18,, Nov. 2003,pp.1293-1301.